

Chapter 3

NiAl and its Alloys

Daniel B. Miracle

Air Force Wright Laboratory, Wright-Patterson AFB, Dayton, OH 45433, USA

Ramgopal Darolia

General Electric Aircraft Engines, 1 Neumann Way, Cincinnati, OH 45215, USA

1. Introduction

NiAl has been studied extensively as a potential structural material in the aerospace industry for over three decades. The attractive attributes of NiAl leading to this interest include a high melting temperature, low density, good environmental resistance, high thermal conductivity, attractive modulus, metal-like properties above a modest ductile-to-brittle transition temperature (DBTT), and low raw materials cost. NiAl can be processed relatively easily by conventional melting, powder, and metal-forming techniques. The two principal limitations of unalloyed NiAl are poor toughness and damage tolerance at room temperature (RT), and inadequate strength and creep resistance at elevated temperature. In spite of these limitations, the payoffs associated with the successful development of NiAl are substantial. The reduced density alone may produce a 30% reduction in the weight of a typical turbine rotor stage (turbine blades and disk), and the high thermal conductivity provides improved cooling efficiency and a significant reduction in airfoil temperatures and thermal gradients.

Investigations of the mechanical properties of NiAl have been conducted on polycrystalline alloys, single-crystal alloys, and NiAl-based composites. Although basic mechanical properties, such as flow strength and ductility, and the mechanisms of deformation have been studied extensively in polycrystalline NiAl, a comprehensive characterization of the full spectrum of physical and mechanical properties required for advanced

aerospace structural applications has not been undertaken for NiAl polycrystals. In contrast, a comprehensive, intensive, and focused activity with the specific goal of developing NiAl single crystals for structural applications in turbine engines has been undertaken. While both polycrystalline NiAl and NiAl single crystals will be discussed in this chapter, the emphasis in the present work reflects the level of understanding and the potential for near-term success with respect to structural applications of NiAl single crystals in gas-turbine engines. NiAl composite materials will be covered in Chapter 13 of this volume by Miracle and Mendiratta.

The goal of this chapter is to provide a focused, critical discussion and assessment of the development activity aimed at establishing NiAl as a high-temperature structural material in turbine engines. Science-based issues and engineering concerns which limit the application of NiAl will be discussed, along with creative approaches to overcoming the identified deficiencies. Insight gained from studies of deformation and failure mechanisms will be provided. In the following section, the physical and mechanical properties of NiAl (stoichiometric and nonstoichiometric) and NiAl alloys will be discussed, and will be compared with the requirements for advanced aerospace structural components (primarily blades and vanes in the high- and low-pressure turbine sections). Specific design considerations dictated by the properties of NiAl will be described in Section 3, and the issues of processing, machining, and component fabrication will be discussed in Section 4. Unless

otherwise stated, compositions will be given in atom % (at %).

2. Physical and Mechanical Properties of NiAl

While it is clear that a 'balance of properties' is required for structural applications in gas-turbine engines, this phrase is often interpreted to emphasize ductility (as a measure of damage tolerance) and strength. However, a stringent balance of a broad range of physical and mechanical properties is required for a successful turbine engine airfoil material, including high melting temperature, low density, moderate stiffness, high thermal conductivity, excellent damage tolerance (even at very high impact rates), good strength, good high- and low-cycle fatigue resistance, and environmental resistance. In addition to satisfying the above physical and mechanical requirements, a new material must address the practical considerations of processibility, machinability, fabrication, and cost effectiveness to compete successfully with existing materials. In this section, the principal physical and mechanical properties of binary and alloyed NiAl will be presented, and will be discussed with respect to the requirements for turbine blades and vanes. Many of the properties of NiAl are linked closely to the crystal structure and the high degree of long-range order, and so a brief review of the bonding, crystal structure, and phase stability is provided.

2.1 Physical Properties

2.1.1 Bonding, Crystal Structure, and Phase Stability

The electronic band structure of stoichiometric NiAl has been calculated using a variety of computational techniques (Lui *et al.*, 1990 and references therein), and the results of these calculations present evidence of strong Ni *d*-Al *p* hybridization along $\langle 111 \rangle$ directions between nearest neighbor Ni-Al atom pairs. Experimental measurements of the electron distribution show a number of features (Fox and Tabernor, 1991). A depletion of electrons occurs at both the Ni and Al sites, as well as from regions midway between next-nearest neighbors along $\langle 100 \rangle$ directions. Associated with these regions of electron depletion is a concomitant increase in electron density between nearest neighbor Ni-Al atom pairs along $\langle 111 \rangle$ directions. The strong Ni *d*-Al *p* hybridization and the buildup of electrons suggest a strong covalent bond along $\langle 111 \rangle$ directions between nearest neighbor Ni-Al atom pairs, and a weak ionic

repulsion between second-nearest neighbor atoms along $\langle 100 \rangle$ is suggested by the experimental observations. These directional bonds are superimposed over a metallic bond. The strong atomic bond along $\langle 111 \rangle$ and the weak bond along $\langle 100 \rangle$ are suggested to produce the observed elastic anisotropy of NiAl and the small shear constant C' . Further, the strength of the Ni-Al bond is qualitatively consistent with the large heat of formation (-72 kJ mol^{-1}) (Dannohl and Lukas, 1974; Henig and Lukas, 1975), the high congruent melting temperature of 1911 K (1638 °C) at the stoichiometric composition (Figure 1) (Nash *et al.*, 1991), the low degree of intrinsic disorder in NiAl (Neumann *et al.*, 1976; Ettenberg *et al.*, 1970), and the presence of short-range order in molten NiAl (Ayushina, 1969; Petrushevskii *et al.*, 1971).

NiAl possesses the ordered cubic B2 (cP2) CsCl crystal structure, which consists of two interpenetrating primitive cubic cells, where Al atoms occupy the cube corners of one sublattice and Ni atoms occupy the cube corners of the second sublattice (Figure 2). NiAl is strongly ordered, even above $0.65T_m$, with an intrinsic disorder parameter of less than 5×10^{-3} (Neumann *et al.*, 1976; Ettenberg *et al.*, 1970). The B2 structure is stable for large deviations from stoichiometry (Figure 1), and significant long-range order is reported for both Ni-rich and Al-rich compositions (Hughes *et al.*, 1971; West, 1964). Deviations from stoichiometry are accommodated by a variable defect structure, where excess Ni atoms occupy Al sites in Ni-rich compositions, and Al-rich compositions result by the formation of vacant Ni sites (Bradley and Taylor, 1937; Taylor and Doyle, 1972). Thermal defects are proposed to involve two lattice sites, and an asymmetric triple defect involving three lattice sites has also been proposed (Wasilewski, 1968). However, it has not been shown that the triple defect occurs in a strongly ordered compound such as NiAl (Miracle, 1993). Additional information on point defects in ordered alloys is provided in Chapter 23 of Volume 1 by de Novion. A martensitic transformation occurs after quenching Ni-rich NiAl (Guard and Turkalo, 1960). NiAl martensite has been reported to possess either a crystal structure related to the face-centred tetragonal $L1_0$ (tP4) structure (Rosen and Goebel, 1968; Enami *et al.*, 1973) or a unique rhombohedral unit cell with 7R stacking in the Ramsdell notation (Tanner *et al.*, 1990). The M_s temperature rises sharply with increasing Ni content, and varies from about 0 K for Ni-40% Al to 1000 K for Ni-32% Al (Smialek and Hehemann, 1973; Chakravorty and Wayman, 1976a; Au and Wayman, 1972). The three requirements for a material to possess the reversible

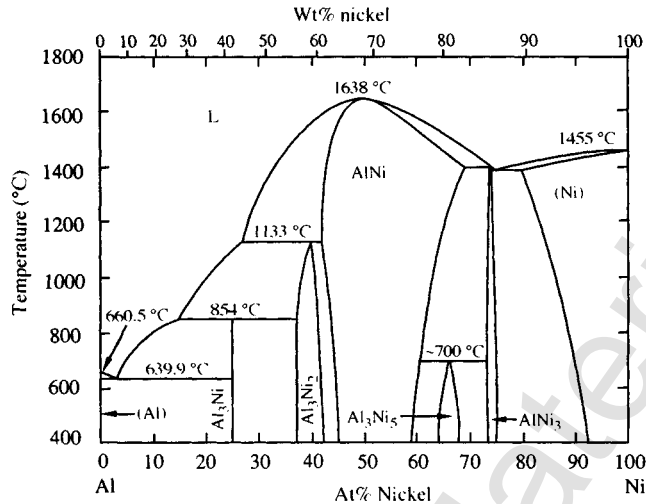


Figure 1. The binary Ni–Al phase diagram from Nash, Singleton, and Murray (1991)

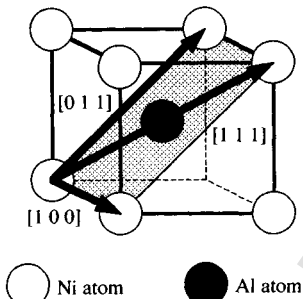


Figure 2. The B2 (cP2) crystal structure (space group $Pm\bar{3}m$, CsCl prototype) of NiAl, with the observed $a(100)$, $a(110)$ and $a(111)$ slip vectors shown on the (011) slip plane

shape memory effect have been shown to occur in NiAl: (i) the martensitic transformation is thermoelastic (Smialek and Hehemann, 1973; Chakravorty and Wayman, 1976a); (ii) the parent and product phases are ordered (Rosen and Goebel, 1968; Enami *et al.*, 1973); and (iii) the martensite is internally twinned (Enami *et al.*, 1973; Chandrasekaran and Mukherjee, 1974; Chakravorty and Wayman, 1976b). These findings are consistent with the observed reversible shape memory effect in NiAl (Enami and Nenno, 1971; Nagasawa *et al.*, 1974). Additional information on the shape memory effect is provided in Chapter 25 of this volume by Schetky.

2.1.2 Density

The density of nonstoichiometric NiAl ranges from 5.35 g cm^{-3} at the Al-rich boundary of the NiAl phase

field to 6.50 g cm^{-3} at the Ni-rich boundary (Bradley and Taylor, 1937; Taylor and Doyle, 1972; Rusovic and Warlimont, 1977; Harmouche and Wolfenden, 1987). The density of binary NiAl at the stoichiometric composition (5.85 g cm^{-3}) is roughly two thirds that of typical Ni-based superalloys, and this provides one of the major benefits of NiAl as an aerospace structural material. The decreased density results in lower self-induced stresses in rotating turbine airfoils, and the turbine disks may be downsized to reflect the lower operating stresses imposed by the reduced mass of the blades. The total reduction in weight for the turbine rotor stage (blades plus disk) is projected to range from 30 to 40% (Darolia, 1991; Darolia *et al.*, 1992a), which represents a decrease of up to 50 kg per rotor stage in a typical turbine engine. This decrease in weight has a cascading effect, whereby the mass of other support structures, such as shafts and bearings, may similarly be reduced. As an added performance benefit, lower weight blades and disks result in lower inertial mass for rotating parts, providing better engine acceleration. The decreased density of NiAl also offers an increased level of flexibility to airfoil designers, whereby increased wall thickness leading to reduced stresses and increased life may be considered, while still providing a weight reduction over existing turbine airfoil materials. In addition, a lower density provides a higher natural frequency of vibration for a given airfoil geometry, so that vibrational modes may be avoided which otherwise would be excited for a particular operational regime.

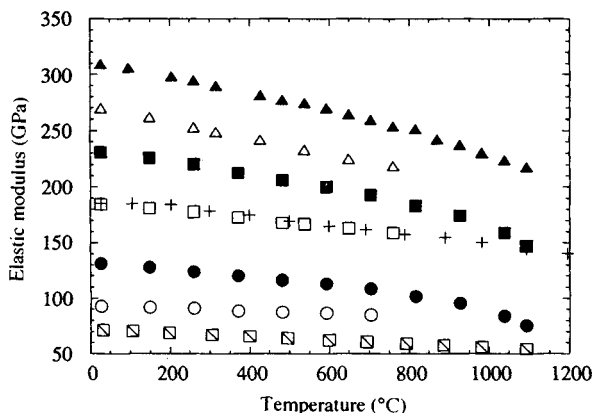


Figure 3. Young's modulus as a function of temperature for single-crystal NiAl along the $\langle 100 \rangle$ (\circ), $\langle 110 \rangle$ (\square), and $\langle 111 \rangle$ (\triangle) directions (Wasilewski, 1966), and for a single-crystal, Ni-based superalloy along the $\langle 100 \rangle$ (\bullet), $\langle 110 \rangle$ (\blacksquare), and $\langle 111 \rangle$ (\blacktriangle) directions (Lahrman and Darolia, 1992). The Young's modulus (+) and shear modulus (\square) of polycrystalline NiAl are also provided (Moose, 1991)

2.1.3 Melting Temperature

Significant improvements in engine cycle efficiency are made possible by increasing the operating temperature of materials in the gas path. Stoichiometric NiAl has a congruent melting temperature of 1638 °C, which is nearly 300 °C higher than the melting temperature of conventional Ni-based superalloys. Nonstoichiometric compositions possess a reduced melting temperature (Figure 1), but still maintain an advantage over current airfoil materials. Melting temperature not only specifies the physical upper limit on use temperature, but also defines the homologous temperature scale, which dictates the temperature at which diffusion-controlled deformation mechanisms begin to dominate. Bulk diffusion in body-centered cubic (b.c.c.) and ordered b.c.c. derivative structures, such as NiAl, typically becomes important above $0.5T_m$ (680 °C), leading to poor high-temperature creep and stress-rupture behavior of binary NiAl. Therefore, while the higher melting temperature of NiAl may provide an opportunity for higher operating temperatures, additional strengthening mechanisms must be developed to utilize this advantage. This will be discussed in more detail in Section 2.2.3 on the creep and stress-rupture behavior of NiAl.

2.1.4 Modulus

A high elastic modulus is often considered to be beneficial in aerospace applications, since service loads

produce smaller elastic deflections. In addition, a higher modulus of elasticity influences the frequency of harmonic vibrations, and a higher modulus increases the natural frequency of vibrations, thereby possibly avoiding vibrational modes at the highest rotational speeds. However, smaller elastic deflections and higher natural frequencies may also be achieved by increasing the section modulus of the airfoil shape. Thermally induced stresses are directly proportional to the elastic modulus, and so larger thermal stresses are produced in a material with a higher modulus for a given thermal gradient. Since thermal fatigue is one of the primary modes of failure in a turbine airfoil, a lower modulus is desirable to improve the thermal fatigue resistance.

Young's modulus of polycrystalline, stoichiometric NiAl at room temperature (188 GPa) (Moose, 1991; Rusovic and Warlimont, 1979) is slightly lower than the Young's moduli of transition metals such as Fe, Co, and Ni (200–210 GPa) and Ni-based superalloys. However, the modulus of NiAl exhibits a reduced sensitivity to temperature, dropping about 2% at 100 °C (Figure 3) (Wasilewski, 1966), compared to 2.4 to 3.2% for the same transition metals. In addition, the lower density of NiAl offsets this lower modulus of NiAl in rotating (self-loading) parts. The modulus of polycrystalline binary NiAl is reported to be relatively insensitive to composition within 6% of the stoichiometric composition (Harmouche and Wolfenden, 1987; Rusovic and Warlimont, 1979), but the single-crystal elastic constants show a significant temperature dependence (Rusovic and Warlimont, 1977). The Young's modulus of NiAl single crystals is highly anisotropic (Figure 3), and the ratio of $E_{\langle 111 \rangle} / E_{\langle 100 \rangle}$ is nearly 2.9 for NiAl at RT, compared to a value of 2.4 for a typical Ni-based superalloy (Lahrman and Darolia, 1992). However, this ratio attains a value of about 2.6 for both NiAl and the Ni-based superalloy at 980 °C. The shear modulus G for polycrystalline NiAl is also given in Figure 3 (Moose, 1991). The temperature dependence of Poisson's ratio for NiAl has been calculated from the Young's modulus and the shear modulus, and is given as

$$\nu = 0.307 + 2.15 \times 10^{-5} T$$

where T is the temperature in Kelvin (Moose, 1991).

2.1.5 Thermal Conductivity

Thermal conductivity influences the design and application of airfoil materials in two ways. First, more efficient

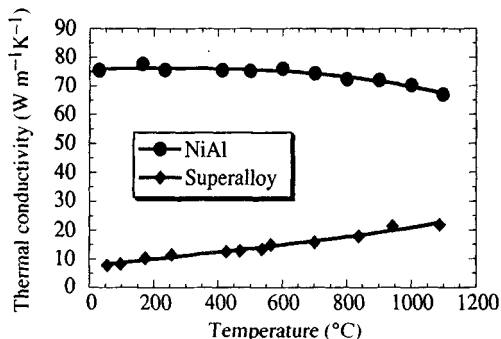


Figure 4. The thermal conductivity of NiAl single crystals as a function of temperature. Data for a typical Ni-based superalloy are provided for comparison (Darolia, 1991)

airfoil cooling is achieved with the rapid heat transfer afforded by high thermal conductivity, providing either a lower metal temperature or a reduction in the amount of cooling air required. The peak temperature for a typical NiAl turbine airfoil may be reduced by as much as 50 °C compared to an Ni-based airfoil using an equivalent amount of cooling air (Lahrman and Darolia, 1992; Darolia *et al.*, 1992). Higher thermal conductivity also produces lower thermal gradients. This reduces the magnitude of thermally induced stresses, since thermal stresses are directly proportional to the thermal gradients.

The thermal conductivity of NiAl is 70–80 W m⁻¹K⁻¹ over the temperature range 20–1100 °C (Darolia, 1991). This is three to eight times larger than the thermal conductivity of Ni-based superalloys (Figure 4), and about one third that of Al. While the overall bulk airfoil temperature may be expected to increase slightly, the thermal gradients are reduced significantly (Lahrman and Darolia, 1992), resulting in lower thermal stresses and improved thermal fatigue. However, the higher thermal conductivity of NiAl may result in higher heat loads to the disk. Alloying tends to reduce the thermal conductivity of NiAl, but significant advantages over Ni-based superalloys are retained (Walston, 1992a; Walston and Darolia, 1993).

2.1.6 Environmental Resistance

High-temperature structural components of advanced aerospace systems typically require service in an oxidizing environment, and this is especially true for turbine airfoils. Resistance to hot salt corrosion and sulfidation is also required. Environmental attack leads to degradation of mechanical properties, and compromises the structural integrity of turbine airfoils, especially in areas with thin cross-sections. NiAl forms the basis of a family

of high-temperature, oxidation-resistant and corrosion-resistant alloys which have been used as coatings on Ni-based and Co-based superalloys in gas-turbine engines over the past 30 years (Goward, 1970; Boone and Goward, 1970). Binary NiAl forms a continuous, protective layer of alumina over a range of temperatures and compositions in the single-phase field (Hutchings and Loretto, 1978). The parabolic rate constant is very low, even in compositions with up to 60 at% Ni, and is typically two orders of magnitude lower than for typical Ni-based superalloys (Barrett, 1988; Smialek and Meier, 1987; Doychak *et al.*, 1989). The oxidation rate in binary compositions is relatively independent of the crystallographic orientation of the oxidized surface on single crystals (Jedlinski and Mrowec, 1987). A variety of alloying additions have been applied to improve performance in static and cyclic oxidation. A significant improvement in oxidation resistance by addition of 0.1% Zr is noteworthy (Barrett, 1988). NiAl has not been shown to exhibit a pest phenomenon. While NiAl is significantly better in environmental resistance than Ni-based superalloys, it has not yet been determined that NiAl alloyed for improved mechanical properties will possess adequate environmental resistance to operate uncoated. It should be mentioned that the coatings used on virtually all turbine blades and vanes are essentially NiAl which has been modified by diffusion of alloying elements from the underlying superalloy, such as Cr, Ti, Mo, W, and Ta.

The rate of sulfidation attack is also parabolic for binary NiAl, and is several orders of magnitude faster than the oxidation of NiAl (Mrowec *et al.*, 1989). The hot-corrosion resistance of unalloyed NiAl is inferior to that of many conventionally cast Ni-based superalloys and is comparable to the newer single-crystal alloys. The corrosion resistance of NiAl can be increased substantially by small additions of Cr and Y (McCarron *et al.*, 1976). The reader is referred to the chapters on oxidation (Doychak, Chapter 43) and corrosion (Duquette, Chapter 42) in Volume 1 for more detailed information.

2.1.7 Coefficient of Thermal Expansion

The coefficient of thermal expansion (CTE) is important for structural applications since thermal stresses depend directly on the magnitude of the CTE. The CTE of NiAl is comparable to that typical for Ni-based superalloys, and is $15.1 \times 10^{-6} \text{ K}^{-1}$ from 820 °C to 1560 °C for stoichiometric NiAl (Wachtell, 1952). Deviations from stoichiometry and minor alloying additions have little influence on the CTE (Rusovic and Warlimont, 1977; Clark and

Whittenberger, 1984; Walston, 1992b; Walston and Darolia, 1993).

2.2 Mechanical Properties

The defect structures and mechanisms of deformation have a strong influence on the mechanical properties of NiAl and their anisotropy in single crystals. These are briefly outlined below to provide a basis for discussion of the mechanical properties of NiAl.

NiAl has a low formation energy for thermal vacancies, and up to 2% of the lattice sites are vacant near the melting temperature (Epperson *et al.*, 1978; Parthasarathi and Fraser, 1984). In addition to these thermal point defects, a large concentration of constitutional point defects (of the order of several % of the lattice sites) is possible in NiAl. As stated earlier, deviations from stoichiometry are accommodated by a variable defect structure, where excess Ni atoms occupy Al lattice sites in Ni-rich NiAl and Ni vacancies form in Al-rich compositions. These constitutional defects have been suggested to form clusters with short-range order, which may act as nuclei for phases adjacent to NiAl (Fox and Tabbernor, 1991; Taylor and Doyle, 1972), and may strengthen nonstoichiometric NiAl (Lasalmonie *et al.*, 1979).

$a\langle 100 \rangle$ is the primary Burgers vector in NiAl, and this slip vector operates on the $\{100\}$ and $\{110\}$ planes (see Figure 2) (Ball and Smallman, 1966a; Kim, 1991; Field *et al.*, 1991a). Although $a\langle 100 \rangle$ screw dislocations are elastically unstable, these dislocations may be stabilized under stress, allowing profuse cross slip to occur (Loretto and Wasilewski, 1971). The critical resolved shear stress (c.r.s.s.) for $a\langle 100 \rangle$ dislocations on $\{110\}$ planes is about 70 MPa in nominally stoichiometric, binary NiAl at RT (Wasilewski *et al.*, 1967; Ball and Smallman, 1966b; Pascoe and Newey, 1968), but there is zero resolved shear stress on these preferred dislocations for single crystals deformed along a $\langle 100 \rangle$ axis. These cube-oriented single crystals are called 'hard' crystals, since they have anomalously high flow stress. The compressive plastic deformation of 'hard' crystals occurs by the motion of $a\langle 111 \rangle$ dislocations on $\{110\}$ or $\{112\}$ planes below 300 °C (Loretto and Wasilewski, 1971; Veysi ere and Noebe, 1992; Campany *et al.*, 1973; Kim, 1991), and is accompanied by the activation of $a\langle 110 \rangle$ dislocations on $\{110\}$ planes above this temperature (Miracle, 1991; Field *et al.*, 1991b; Kim, 1991). $a\langle 111 \rangle$ dislocations are not typically observed in 'hard' crystals tested in tension below 300 °C (Darolia *et al.*, 1992). The c.r.s.s. for $a\langle 111 \rangle$ dislocations is about 600 MPa at RT (nearly 1% of the

shear modulus), and drops only slightly at 300 °C to about 575 MPa (Pascoe and Newey, 1968). $a\langle 110 \rangle$ dislocations begin to operate above 300 °C (Miracle, 1991; Kim, 1991; Field *et al.*, 1991b), and the c.r.s.s. for these dislocations drops rapidly with increasing temperature from about 575 MPa at 300 °C to less than 100 MPa above 700 °C (Miracle, 1993 and references therein). Above 700 °C, an analysis of the available evidence suggests that NiAl deforms by diffusional processes (Miracle, 1993).

It has been suggested that a reduction of the $a/2\langle 111 \rangle$ antiphase boundary (APB) energy will favor the activation of $a\langle 111 \rangle$ dislocations, providing the five independent slip systems necessary for polycrystalline ductility (Rachinger and Cottrell, 1956). A number of computational algorithms have been applied to calculate this quantity in NiAl, and to assess the influence of ternary additions on the APB energy. Calculations using the embedded atom method (for a discussion of this technique, see Voter, Chapter 4 in Volume 1) provide APB energies ranging from 240 to 460 mJ m⁻² (Clapp *et al.*, 1989; Rao *et al.*, 1991), while first-principles calculations predict values near 900 mJ m⁻² (Fu and Yoo, 1991; Hong and Freeman, 1991a). *Ab initio* calculations suggest that large additions of ternary elements, such as Cr and Mn, as well as large deviations from stoichiometry, significantly reduce the APB energy of NiAl (Hong and Freeman, 1991a,b). Shear-induced planar defects, such as APBs, have not been observed in NiAl, and an experimentally determined lower bound on the APB energy ranges from 500 to 750 mJ m⁻² (Veysi ere and Noebe, 1992). Thus, the high APB energy in NiAl has been suggested to contribute to the difficulty in moving non- $a\langle 100 \rangle$ dislocations. Further discussion of planar defects in NiAl is provided elsewhere (Miracle, 1993), and the reader is also referred to Chapter 21 by Sun in Volume 1.

2.2.1 Ductility

The RT tensile ductility of polycrystalline binary NiAl can range from 0 to 2%, depending upon stoichiometry (Hahn and Vedula, 1989), texture (Hahn and Vedula, 1989; Vedula *et al.*, 1989), grain size (Schulson and Barker, 1983), and possibly impurity content and substructure. The $\langle 100 \rangle$ slip direction provides only three independent slip systems, and this limitation has been used to explain the lack of significant RT tensile plasticity in polycrystalline NiAl. Above the DBTT of about 400 °C, polycrystalline NiAl becomes very ductile, and plastic elongations of over 40% are observed at 600 °C (Hahn and Vedula, 1989). Additional slip systems

have not been verified to operate in NiAl polycrystals, and it has been proposed that both climb and glide are responsible for the ductility of polycrystalline NiAl up to about 800 °C (Hahn and Vedula, 1989; Miracle, 1993). Above 800 °C, diffusion-assisted processes are likely to control the deformation of polycrystalline NiAl (Miracle, 1993).

The RT tensile ductility of binary NiAl single crystals is anisotropic. 'Hard' single crystals fail after only elastic strains, while other orientations (termed 'soft' crystals), such as $\langle 110 \rangle$ and $\langle 111 \rangle$, possess up to 2% plastic deformation (Lahrman *et al.*, 1991). In compression, 'hard' single crystals typically deform by 'kinking', an extremely localized shear instability which occurs by the glide of $\alpha(100)$ dislocations (Fraser *et al.*, 1973a; Fraser *et al.*, 1973b). Again, the plastic behavior is highly sensitive to stoichiometry and interstitial content. Potential factors limiting ductility in single crystals include inadequate dislocation sources, low dislocation mobility, inhomogeneous slip, and low fracture stress. Each of these have been postulated to explain the brittle failure of 'hard' single crystals, and it is uncertain as to what extent these may apply to the deformation of 'soft' single crystals and polycrystals. The DBTT for 'soft' crystals is 200 °C, while 'hard' crystals become ductile just below 400 °C (Lahrman *et al.*, 1991). NiAl single crystals become very ductile above the DBTT, and both 'hard' and 'soft' crystals exhibit more than 20% elongation at 400 °C (Lahrman *et al.*, 1991; Wasilewski, *et al.*, 1967). The dependence of ductility and the DBTT on strain rate is small in both 'hard' and 'soft' single crystals between strain rates of 8.3×10^{-5} and $8.3 \times 10^{-3} \text{ s}^{-1}$ (Lahrman *et al.*, 1991). However, the ductility of NiAl at impact strain rates has not been determined.

While fundamental concepts exist which address potential sources of limited ductility in NiAl, such as poor grain boundary cohesion, an insufficient number of independent slip systems, and slip localization, these concepts do not provide clear guidance on the selection of alloying additions which can modify these effects. Therefore, efforts to improve the intrinsic RT ductility of NiAl have typically been based on empirical reasoning. Boron additions to strengthen NiAl grain boundaries have not succeeded in improving ductility significantly, since B is a potent solid-solution strengthener, and the yield strength of NiAl + B typically exceeds the fracture strength (George and Liu, 1990). Alloying additions to increase the number of independent slip systems by lowering the APB energy have been rationalized in various ways (Field *et al.*, 1991; Law and Blackburn, 1987), and it has been

reported that Cr additions favor the activation of $\alpha(111)$ dislocations (Law and Blackburn, 1987; Miracle *et al.*, 1989; Field *et al.*, 1991c). However, these approaches address a condition that has been found to be necessary but insufficient for ductility. Theoretical and practical approaches which are able to address the basic issues of the nucleation and mobility of a sufficient number of glide dislocations and the homogeneity of slip have not yet been established.

Impurities (especially interstitial elements) are generally considered to have a strong influence on the ductility of intermetallic alloys. While both B and C have been shown to increase the DBTT at levels ≥ 300 p.p.m. by weight (w.p.p.m.) (George and Liu, 1990; Law and Blackburn, 1987; George *et al.*, 1990), no definite effect has been established for most potential interstitial contaminants in NiAl. Typical impurity levels are 40–80 w.p.p.m. for O and C, and 1–5 w.p.p.m. for S, P, and N. However, much higher levels may result from powder processing or careless handling. Although the Si content is expected to be low in polycrystalline material, Si can be as high as 1000 w.p.p.m. in NiAl single crystals due to contamination from the mold material during single-crystal processing.

Microalloying with Fe, Ga, and Mo has recently been shown to improve significantly the RT tensile ductility of NiAl single crystals tested along a $\langle 110 \rangle$ direction, increasing the failure strain from a typical value of 1% for stoichiometric NiAl to as high as 6% for NiAl + 0.25% Fe (Darolia *et al.*, 1992a; Darolia *et al.*, 1992b). The plastic elongation to failure at RT as a function of Fe, Ga, and Mo concentration for the $\langle 110 \rangle$ -oriented specimens is shown in Figure 5(a), and the 0.2% yield strengths are plotted as a function of alloying concentration in Figure 5(b). Solid-solution softening may be occurring in NiAl with Fe and Ga, while solid-solution strengthening is suggested for Mo additions (Figure 5). While the alloys containing Fe and Ga are single phase, the NiAl + Mo alloys contain very small (5–20 nm) α -Mo precipitates, which could explain the increased yield strength in these alloys. Single crystals with 0.25% Fe showed similar increases in plastic strains to failure for other orientations, except for crystals tested along $\langle 100 \rangle$. However, the DBTT of $\langle 100 \rangle$ -oriented single crystals decreased with additions of 0.1% Fe and 0.25% Fe (Darolia *et al.*, 1992b). The slip system is unchanged with these microalloying additions. Even though substantial plastic elongation is observed, the fracture surface still consists of cleavage facets.

The mechanism(s) by which these elements enhance the RT ductility of $\langle 110 \rangle$ NiAl single crystals have not been established, and are only speculative at this point.

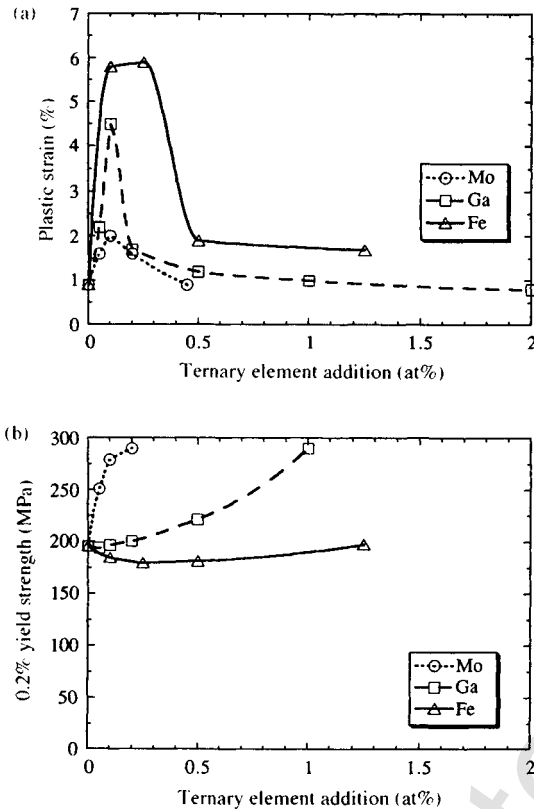


Figure 5. The compositional dependence of (a) ductility, and (b) 0.2% yield strength of NiAl single crystals tested in tension along a $\langle 110 \rangle$ direction at RT (Darolia *et al.*, 1992b)

The c.r.s.s. for $\alpha(111)$ dislocations is not significantly reduced, and transmission electron microscopy (TEM) observations do not suggest the activation of additional slip systems. One speculation is that alloying additions affect the electronic structure and bonding characteristics of NiAl, which may then alter the dislocation core structure, and hence modify dislocation mobility, the Peierls stress, and thermally activated slip processes. Indirect effects, arising from interactions with point defects or impurities in NiAl (particularly interstitial elements such as O, N, C, or S) could also be responsible for the ductility enhancement, as could closer effective approach to precise stoichiometry made possible by substitutional atoms. The large increases in tensile ductility by microalloying are exciting and provide an approach for producing ductile NiAl alloys. It is important to note that many earlier studies investigated alloy additions $\geq 1\%$, where little or no improvement in ductility was measured by Darolia (1991), and additional activity in the area of microalloying may be fruitful.

Alloy additions to polycrystalline NiAl have been largely unsuccessful in producing RT tensile ductility, with the possible exception of small Mo additions (Grala, 1960; Law and Blackburn, 1987; Russell *et al.*, 1991). Although a critical grain size has been postulated below which apparent ductility may be induced by stable microcracking (Schulson and Barker, 1983; Schulson, 1985), an analysis of the available experimental data does not fully support this proposition (Miracle, 1993). It has been shown that extruded NiAl near the stoichiometric composition can exhibit as much as 2% RT tensile elongation (Hahn and Vedula, 1989). This material is strongly textured, but the reasons why a textured material should possess enhanced ductility have not been addressed.

2.2.2 Strength

A turbine airfoil is subjected to stresses from centrifugal loading, thermal stresses from temperature gradients, stresses from the high-velocity gas, and vibrational excitation. Depending on the airfoil design, temperature, and location on the turbine blade, a typical Ni-based superalloy requires a tensile yield strength of approximately 700–1000 MPa at RT, and up to 500 MPa at temperatures as high as 800 °C. The creep and stress-rupture performance, and the high- and low-cycle fatigue resistance, are also strongly dependent on the tensile properties of the airfoil material. Overall, the strength properties of NiAl alloys must at least equal those of older Ni-based superalloys such as René 80, B1900 or MarM 200, which have been used for over 20 years as blade materials. The density and the thermal conductivity advantages would then make NiAl alloys attractive replacements for the newer single-crystal superalloys.

The temperature dependence of the tensile yield strength of single-crystal and polycrystalline stoichiometric NiAl is shown in Figure 6 (Darolia, 1991; Darolia *et al.*, 1992a; Field *et al.*, 1991). The strength is compared with René 80, a conventionally cast, Ni-based superalloy commonly used as a turbine blade material. The yield strength of NiAl polycrystals and 'soft' single crystals is too low to be of interest in the stoichiometric, unalloyed state. Although 'hard' single crystals are somewhat more attractive, the strength drops rapidly with increasing temperature. It is obvious that the strength of binary NiAl needs significant improvement to be competitive with Ni-based superalloys. Deviations from stoichiometry can have a potent strengthening effect, and a Ni–40% Al alloy provides a significant strengthening increment in compression up to 700 °C

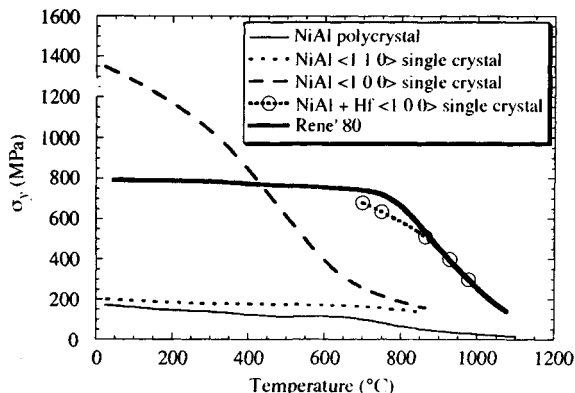


Figure 6. The temperature dependence of the tensile yield strength of binary, polycrystalline NiAl (Rozner and Wasilewski, 1966) and binary NiAl single crystals tested along $\langle 110 \rangle$ (Darolia *et al.*, 1992a) and $\langle 100 \rangle$ (Field *et al.*, 1991b). Data for polycrystalline René 80 (Darolia, 1991) are included for comparison. The strength improvement for NiAl alloyed with Hf tested along a $\langle 100 \rangle$ axis is also shown (Darolia *et al.*, 1992c)

(Bowman *et al.*, 1989). This effect diminishes with increasing temperature, and at 1200 °C stoichiometric NiAl is as strong as nonstoichiometric NiAl (Vandervoort *et al.*, 1966). Stoichiometric and Ni-rich NiAl follow the Hall–Petch relationship

$$\sigma_y = \sigma_0 + kd^{-1/2}$$

and both σ_0 and k increase with increasing deviation from stoichiometry (Schulson and Barker, 1983; Baker *et al.*, 1991). The strain-hardening rate is high below the DBTT, but decreases significantly above this temperature (Hahn and Vedula, 1989; Raj *et al.*, 1989; Ball and Smallman, 1966b; Rozner and Wasilewski, 1966; Lautenschlager *et al.*, 1965). Disagreement exists between different studies concerning the effect of strain rate on the yield strength of NiAl at different temperatures, but drastic changes in strength are not observed under strain rates from roughly 10^{-2} to 10^{-4} s^{-1} (Lahrman *et al.*, 1991; Wasilewski *et al.*, 1967; Pascoe and Newey, 1968).

The high-temperature strength of NiAl may be improved by solid-solution strengthening, precipitate strengthening (with metallic, intermetallic, or ceramic particles), elimination of grain boundaries by the single-crystal route, and composite strengthening. NiAl composites will be addressed in Chapter 13 of this volume by Miracle and Mendiratta.

Solid-solution strengthening can be significant even at low levels of the ternary element, especially with

addition of Group IVB and VB elements such as Ti, Hf, Zr, V, and Ta. For example, additions of 0.2% Hf to NiAl can increase the RT tensile strength of a $\langle 110 \rangle$ -oriented specimen from a typical value of 210 MPa for stoichiometric NiAl to 600 MPa (Darolia *et al.*, 1992). Limited low-temperature solubility ($< 1\%$) exists for elements such as Cr, Mo, and Re. When added beyond their solubility limit, these elements precipitate a disordered b.c.c. phase, which strengthens NiAl. Proper solution and aging treatments can result in control of the size and distribution of these precipitates. NiAl ternary alloys with b.c.c. refractory metals often possess a eutectic reaction, and directionally solidified microstructures result in a dramatic increase in high-temperature strength (Stover, 1966), as shown in Figure 7.

Additions of Group IVB or VB elements beyond their solubility limits in NiAl produce several ternary intermetallic compounds, including the $L2_1$ (cF16) Heusler (or β') phase Ni_2AlX , and the primitive hexagonal Laves phase (hP12) NiAlX . These phases can contribute significantly to the strengthening of the NiAl alloys (Rudy and Sauthoff, 1986; Sauthoff, 1989; Polvani *et al.*, 1976). The close relationship between the B2 and $L2_1$ crystal structures (Figure 8) results in coherent or semicoherent precipitates, which can strengthen NiAl alloys to levels equivalent to those of the Ni-based superalloy MarM 200 (Polvani *et al.*, 1976). NiAl alloys strengthened by the Laves phase are more brittle than alloys strengthened by the β' phase, and are more difficult to machine into test specimens. Si contamination (600–1000 w.p.p.m) from mold materials during single-crystal processing results in 10–40 nm cuboidal precipitates of the ordered G phase ($\text{Ni}_{16}\text{X}_6\text{Si}_3$ (cF116), where X is Zr or Hf) (Locci *et al.*, 1991). These precipitates are coherent with NiAl and are fairly resistant to coarsening. The G phase is known to have attractive high-temperature properties (Westbrook, 1956), and it is possible that the G phase contributes to strengthening in NiAl. However, its exact role needs further exploration. Significant potential exists for further improvement in strength (and perhaps ductility and toughness) by careful development of the volume fraction and morphology of the β' precipitates in NiAl, similar to the development of $\gamma-\gamma'$ Ni-based superalloys. A fundamental, systematic study of the precipitate volume fraction, morphology, lattice mismatch and coherency strains, size effects, precipitate stability, and solid-solution contributions is warranted. NiAl alloys strengthened with incoherent dispersoids such as Al_2O_3 , TiB_2 and HfC are being developed by various research groups (Whittenberger and Viswanadham 1989; Jha *et al.*,

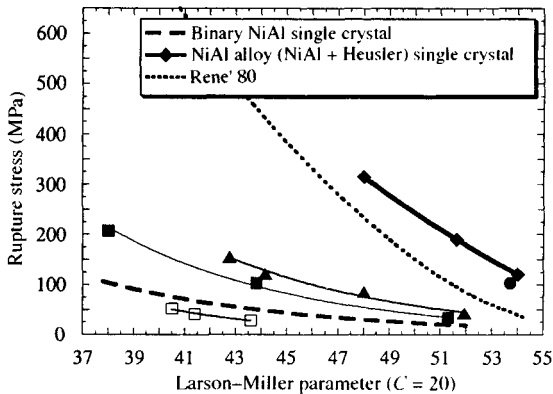
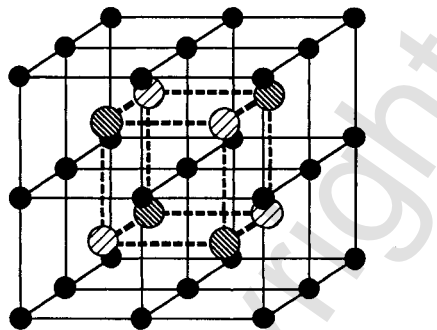


Figure 7. The stress-rupture properties of NiAl and NiAl alloys. The Larson–Miller parameter is calculated as $P = (T_R/1000)(\log t + 20)$, where T_R is the absolute temperature in Rankine, and t is the time in hours. The data are for binary polycrystalline NiAl (\square) (Grala, 1960), and alloys of NiAl + 9% Mo aligned eutectic (\bullet) (Stover, 1966), NiAl + 6 vol% ThO_2 (\blacksquare) (Seybolt, 1966), and NiAl + 20 vol% TiB_2 (\blacktriangle) (Kumar, 1991). The dashed lines are from Figure 12 of Darolia (1991). The line for the NiAl single-crystal alloy with Heusler precipitates represents the upper bound of a range of data (Darolia *et al.*, 1992a; Darolia *et al.*, 1992b), and this alloy is equivalent to the single-crystal, Ni-based superalloy René N4



Structure	Compound	\bullet	⦿	⦿
B2	NiAl	Ni	Al	Al
L2 ₁	Ni ₂ AlTi	Ni	Ti	Al
D0 ₃	Fe ₃ Al	Fe	Fe	Al

Figure 8. Crystal structure of the B2 derivative lattices, illustrating the close relationship between the B2 (cP2) and L2₁ Heusler (cF16, or β') structures

1989; Whittenberger *et al.*, 1990), but these alloys do not yet compete with the β' -strengthened NiAl, as shown in Figure 7 (Kumar *et al.* 1992b).

NiAl single-crystal alloys show dramatic improvements in high-temperature strength over NiAl polycrystals, and their strengths can equal Ni-based, single-crystal

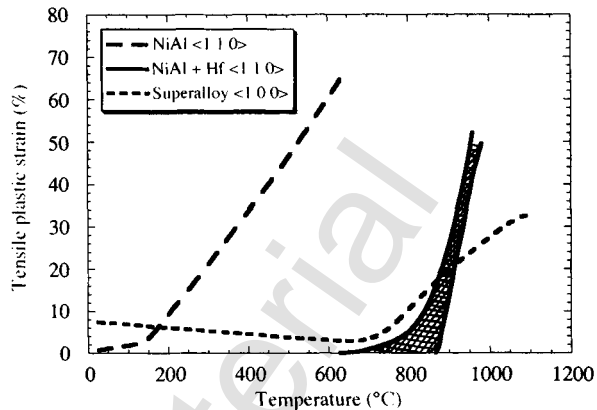


Figure 9. Tensile ductility as a function of temperature typical of strengthened NiAl single-crystal alloys in the cross-hatched area (Darolia *et al.*, 1992a). The ductilities of binary NiAl and a typical Ni-based superalloy are shown for comparison

strength levels (Figures 6 and 7). Accounting for the higher thermal conductivity and lower density of NiAl (the stresses in Figure 6 and 7 are not corrected for density), these NiAl alloys are attractive replacements for current single-crystal, Ni-based superalloys.

NiAl single-crystal alloys which possess the best high-temperature strengths are generally less ductile than binary NiAl, have DBTTs which increase substantially as the strength is increased, and possess low fracture toughness values. Figure 9 shows ductility as a function of temperature typical of strengthened NiAl alloys (Darolia *et al.*, 1992c). The high DBTT of strengthened NiAl single-crystal alloys remains an issue which must be resolved through further alloy development or design methodology. Development of intermetallic alloys possessing both RT ductility and sufficient high-temperature strength is a very difficult challenge and may prove to be an elusive goal.

2.2.3 Creep and Stress-rupture

Highly creep-resistant materials are desirable to maintain the aerodynamic shape of the airfoil and a tight clearance between the blade tip and the gas path seal, which controls the cycle efficiency of the turbine engine. Typical creep requirements for a Ni-based superalloy include stresses up to 200 MPa at temperatures as high as 1000 °C for over 300 h. A creep strain of 1% is often considered to constitute a creep failure. Therefore, both the steady-state creep rate and the amount of primary creep strain must be very low for acceptable creep performance. Ni-based superalloys rely on precipitation

Table 1. Summary of creep parameters for NiAl

Al (at%)	Grain size (μm)	Temperature ($^{\circ}\text{C}$)	n	Q (kJ mol^{-1})	Reference
48.25	5–9	723–1123	6–7.5	313	Whittenberger (1988)
49.2	15–20	823–1123	5.75	314	Whittenberger (1987)
50	12	923–1023	6	350	Whittenberger, Arzt, and Luton (1990)
50	450	800–1045	10.2–4.6	283	Yang and Dodd (1973)
50	500	900	4.7		Rudy and Sauthoff (1985)
50.4	1000	802–1477	7–3.3	230–290	Vandervoort, Mukherjee, and Dorn (1966)
50	SX [123]	750–950	7.7–5.4		Hocking, Strutt, and Dodd (1971)
50	SX	750–1055	4–4.5	293	Bevk, Dodd, and Strutt (1973)
50	SX [001]	723–1023	6	440	Noebe and Whittenberger (1991)

SX = single crystal.

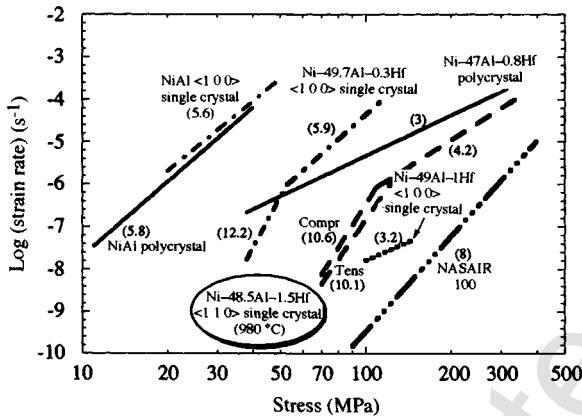


Figure 10. Log (strain rate) versus stress (logarithmic scale) for single-crystal and polycrystalline NiAl at 1023 $^{\circ}\text{C}$ (Whittenberger, 1987; Nathal and Ebert, 1985; Whittenberger *et al.*, 1991; Field, 1991; Nathal, 1992; Locci *et al.*, 1992). The stress exponent n is shown in parentheses. Data for several NiAl + Hf alloys and for the Ni-based superalloy NASAIR 100 are included for comparison (Compr = compression testing; Tens = tensile testing) (Darolia *et al.*, 1992)

strengthening to allow operation at 85% of their homologous melting temperature (~ 1150 $^{\circ}\text{C}$), while binary NiAl, being a b.c.c.-derivative structure, does not have useful creep strength above about 50% of its absolute melting temperature (~ 680 $^{\circ}\text{C}$).

The creep deformation of NiAl can be divided into primary, secondary and tertiary stages, as commonly observed for metals and alloys. The secondary creep rate has been expressed in the form of Dorn's equation

$$\dot{\epsilon} = A\sigma_n \exp(-Q/RT)$$

where σ is the applied stress, n is the stress exponent, Q is the activation energy for creep, R is the gas constant, T is the absolute temperature, and A is a constant related to the structure of the material. A summary of reported

creep parameters for binary NiAl is presented in Table 1 (from Nathal, 1992), and a comparison of the creep behavior of NiAl single crystals and polycrystals is presented in Figure 10 (Whittenberger, 1987; Nathal and Ebert, 1985; Whittenberger *et al.*, 1991; Field, 1991; Nathal, 1992; Locci *et al.*, 1992). An analysis of data in the literature for the stress exponent n , substructural observations, and activation energies clearly establish the role of diffusional processes in the creep of binary NiAl above about 900 $^{\circ}\text{C}$ (Miracle, 1993). The exponent n appears to depend on orientation in single crystals (Forbes *et al.*, 1992). Although the scatter in n makes it difficult to specify with confidence a particular deformation mechanism (for example, dislocation climb versus viscous glide), a recently developed strain rate change test has shown that Ni-rich NiAl exhibits 'pure metal' behavior between 800–1000 $^{\circ}\text{C}$, indicating that dislocation substructure (climb, with $n = 5$), rather than lattice friction (viscous glide, or solute drag, with $n = 3$) controls deformation in this temperature range (Yaney and Nix, 1988). Deformation appears to be controlled by viscous glide of dislocations above 1200 $^{\circ}\text{C}$ (Miracle, 1993 and references therein). Although considerable scatter exists, the activation energy has been assessed to be between 250 and 300 kJ mol^{-1} (Miracle, 1993), which agrees reasonably well with the activation energy for the diffusion of ^{63}Ni in stoichiometric NiAl (Hancock and McDonnell, 1971).

The high-temperature deformation properties of binary, stoichiometric NiAl single crystals have recently been studied systematically as a function of orientation in tensile creep and in constant-strain-rate compression tests at temperatures between 850 and 1200 $^{\circ}\text{C}$ (Forbes *et al.*, 1992). The samples exhibited a strong orientation dependence in the strength as well as in other deformational characteristics. 'Soft' single crystals reach a steady state rapidly and develop little dislocation substructure. Deformation in these crystals is also characterized by

Table 2. Dependence of n on temperature and orientation

Temperature (°C)	Polycrystals ^a	[223]	[111]	[110]	[001]
850	6.9–10.1	7.0	5.5	7.2	11.4
1000	4.9–6.5	4.6	4.7	6.0	4.7
1200	3.8–4.0	4.6	4.5	4.5	3.8

^aPolycrystal data from Yang and Dodd (1973), Vandervoort, Mukherjee, and Dorn (1966), and Whittenberger (1987).

an activation energy which is significantly below that for volume diffusion in NiAl. These characteristics suggest that deformation in 'soft' crystals is controlled by glide of $a\langle 100 \rangle$ dislocations. However, diffusive aspects of deformation were evident at temperatures above 1000 °C. 'Hard' single crystals show strain hardening even at 1200 °C, and develop an extensive dislocation substructure. The dislocation substructure is composed of $a\langle 100 \rangle$ dislocations which are unstressed for glide in this orientation and can move only by diffusive processes. The creep curves are sigmoidal, also suggesting sluggish dislocation motion. In addition, the activation energy for steady-state creep in the 'hard' orientation is near that for diffusion. In contrast to deformation in 'soft' crystals, deformation in 'hard' crystals was strongly controlled by climb. The stress exponents for the various temperatures and orientations are presented in Table 2. The orientation dependence of the stress exponent is clearly evident at 850 °C from the data in Table 2. Overall, the stress exponents show a temperature dependence similar to polycrystalline NiAl.

The creep resistances of NiAl alloys have followed the improvements in the high-temperature tensile and stress-rupture strengths (Figure 10). Several conclusions can be drawn from Figure 10. As expected, single-crystal NiAl has better creep resistance than polycrystalline NiAl of the same composition. Significant improvement in creep resistance is obtained with the addition of Hf to NiAl, and the creep resistance of a single-crystal NiAl alloy containing 1% Hf approaches that of a Ni-based single-crystal superalloy. The stress exponents of the single-crystal alloys appear to depend upon the alloy composition and stress, though it is not clear why the 1.5% Hf alloy, which has a higher volume fraction of the Heusler phase, has a lower n than the 1.0% Hf alloy. At lower stresses, the stress exponents for single-crystal NiAl alloys ($n \approx 10$) are often much higher than those of polycrystalline alloys, and can match those for single-crystal, Ni-based superalloys. This implies that creep is not controlled by simple diffusional processes, and the dislocation/particle interactions responsible for the excellent creep resistance of superalloys may be

controlling the creep resistance. There appears to be no difference in creep behavior whether the creep test is conducted under constant load or constant velocity (Whittenberger, 1987; Nathal, 1992; Nathal and Ebert, 1985; Whittenberger *et al.*, 1991; Locci *et al.*, 1992; Field, 1992a). However, it is surprising to note that the tensile creep rates appear to be nearly half an order of magnitude lower than the compressive creep rates.

Limited work indicates that the creep behavior and stress-rupture strengths are highly anisotropic in NiAl single crystals (Field, 1992b). The steady-state creep rate in 'hard' crystals can be as much as half an order of magnitude lower than along $\langle 110 \rangle$ and $\langle 111 \rangle$ 'soft' orientations, and this may result from the competition between the viscous glide of $a\langle 100 \rangle$ dislocations in 'soft' crystals ($n = 3$), and the climb of $a\langle 100 \rangle$ dislocations in 'hard' crystals ($n = 5$). With the limited data available, it is difficult to comment on the operative creep mechanisms, and further work with various alloy compositions and test conditions is needed.

2.2.4 Fracture Properties

The fracture mode of binary, polycrystalline NiAl is primarily intergranular at RT (Hahn and Vedula, 1989; Locci *et al.*, 1992; George and Liu, 1990; Law and Blackburn, 1987; Lewandowski *et al.*, 1990), changes to transgranular cleavage around 400–500 °C (Hahn and Vedula, 1989; Law and Blackburn, 1987), and occurs by ductile rupture above 600 °C (Hahn and Vedula, 1989). Transgranular cleavage is favored at RT in notched samples (Rigney *et al.*, 1989; Kumar *et al.*, 1992a), in nonstoichiometric NiAl (Nagpal *et al.*, 1991; Vehoff, 1992), and in coarse-grained NiAl fractured at a high strain rate (Guard and Turkalo, 1960). Additions of ≥ 30 w.p.p.m. B suppress intergranular fracture in stoichiometric NiAl at RT (George and Liu, 1990; Law and Blackburn, 1987; George *et al.*, 1990), but 300 w.p.p.m. C does not (George and Liu, 1990). Fracture in NiAl single crystals does not occur on a single cleavage plane, and several crystallographic facets are often seen. For example, fracture initiates on $\{115\}$ or $\{117\}$ planes prior to final fracture on $\{110\}$ planes in notched, single-crystal bend specimens stressed along a $\langle 110 \rangle$ direction (Chang *et al.*, 1991). Low-index fracture planes, such as $\{115\}$, $\{117\}$, $\{123\}$, and $\{221\}$, are often quoted (Schneibel *et al.*, 1992). No evidence of ductile rupture is evident on single-crystal fracture surfaces.

While current design methodology does not specify a minimum requirement for fracture toughness, 50 MPa m^{1/2} is typical for Ni-based superalloys. The

fracture toughness (K_{IC}) of polycrystalline, binary NiAl is 4–6 MPa m^{1/2} at RT for a wide range of grain sizes (Kumar *et al.*, 1992a; Russell *et al.*, 1991; Reuss and Vehoff, 1990). For zone-refined NiAl, K_{IC} increases from about 5 MPa m^{1/2} at RT to 50 MPa m^{1/2} at 400 °C, whereas K_{IC} increases only to 10 MPa m^{1/2} at 400 °C for as-cast material (Reuss and Vehoff, 1990). The fracture toughness in single crystals depends upon specimen configuration, crystallographic direction with respect to loading direction, and the geometry of the notch. K_{IC} for binary, single-crystal bend specimens with a straight notch tested along $\langle 110 \rangle$ is 4–5 MPa m^{1/2} (Vehoff, 1992; Reuss and Vehoff, 1990), and 8 MPa m^{1/2} is obtained for samples tested along $\langle 100 \rangle$ (Chang *et al.*, 1991). RT values of K_{IC} for $\langle 100 \rangle$ samples determined in tension with a chevron-notched sample can be a factor of two higher than the value obtained with a single notch in a bending test (Bain, 1992b). The fracture toughness increases with increasing temperature to about 15 MPa m^{1/2} near 300 °C for $\langle 110 \rangle$ specimens, and increases to about 30 MPa m^{1/2} for $\langle 100 \rangle$ samples. The largest increase in toughness occurs near the DBTT, but the toughness drops, then increases, just above the DBTT for both $\langle 100 \rangle$ and $\langle 110 \rangle$ specimens (Reuss and Vehoff, 1990). The fracture toughness increases with temperature due to increased plasticity at the tip of the growing crack (Chang *et al.*, 1991).

The ductility-improving additions of Fe and Ga, which increase the RT ductility of $\langle 110 \rangle$ single crystals, improve the RT fracture toughness by 50% (Darolia and Chang, 1991), while 50% reduction in the RT fracture toughness is measured in high-strength NiAl alloys (Bain, 1992b). The low toughness of NiAl alloys below the DBTT is a critical issue that must be addressed. The alternative toughening approach of ductile reinforcements in an NiAl matrix is discussed in Chapter 13 of this volume by Miracle and Mendiratta.

Few impact data are available for NiAl, and a value of $6.9 \pm 0.4 \text{ J cm}^{-2}$ is given as the fracture energy of stoichiometric polycrystalline NiAl (Russell *et al.*, 1991), and 0.8 J cm^{-2} is given as the impact energy of unnotched polycrystalline NiAl (Nardone *et al.*, 1990).

2.2.5 Fatigue Behavior

The low-cycle and high-cycle fatigue lives and behavior of NiAl alloys in the $\langle 100 \rangle$ orientation have recently been found to be similar to Ni-based superalloys (Wright *et al.*, 1992; Bain, 1992a). In low-cycle fatigue, an NiAl alloy containing Mo (which showed some RT ductility in $\langle 110 \rangle$ single crystals) was tested at 760 °C in a $\langle 100 \rangle$ orientation (Bain, 1992a). This alloy followed Manson–

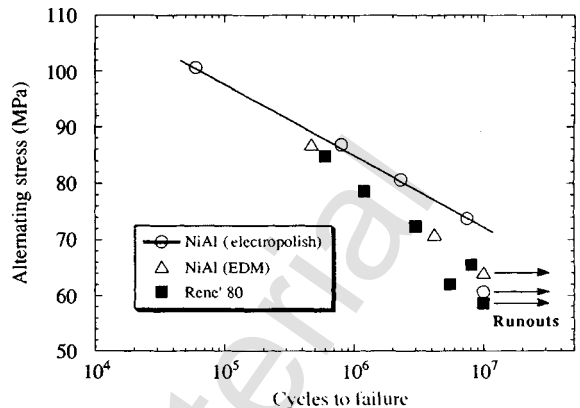


Figure 11. The high-cycle fatigue behavior of a Hf-containing NiAl single-crystal alloy compared to that of René 80 (Wright *et al.*, 1992)

Coffin strain-life behavior, typical of Ni-based superalloys. The low-cycle fatigue lives of an Hf-containing NiAl alloy (with stress-rupture properties equivalent to René 80) are similar to the lives of single-crystal, Ni-based superalloy René N4 at temperatures above as well as below the DBTT of the NiAl + Hf alloy. The high-cycle fatigue behavior of this alloy tested in the $\langle 100 \rangle$ orientation at 980 °C with an R ratio of 0.025 at 30 Hz was found to be equal to René 80 (Figure 11). Electrodischarge machining (EDM), which typically produces a recrystallized layer and surface cracks up to 25 μm deep, did not significantly degrade the high-cycle properties compared to electropolished specimens where cracks and the recrystallized layer were removed. This suggests that the alloy is sufficiently ductile at the test temperature to ameliorate surface-related degradation. With the limited data available, it appears that the fatigue lives of NiAl alloys follow improvements in their strengths.

3. Design of NiAl Airfoils

Each of the physical and mechanical properties discussed in the previous section influence the design of structural components. Of particular importance in the design of turbine airfoils are the issues of limited ductility and damage tolerance, strain-rate sensitivity, and anisotropic properties.

3.1 Ductility and Toughness

Although minimum levels of neither ductility nor toughness are specified in the design of turbine blades,

some amount is desirable for processibility, handling and assembly, component reliability, and attachment to the turbine disk. Plastic accommodation is required to relieve high contact stresses between the airfoil and the turbine disk in the attachment region, especially at radii in the dovetail. Appropriate handling and assembly techniques must therefore be established and verified to enable the use of materials with limited RT ductility, such as NiAl. In the absence of ductility at RT (where engine assembly is accomplished), a compliant material between the NiAl airfoil and the turbine disk may be used to accommodate point stresses. Redesign of the dovetail geometry, such as reducing the number of attachment lobes and increasing their radii, may be employed to reduce the magnitude of stress concentrations. In addition, the anisotropic elastic and plastic properties of NiAl offer unique challenges for the design of turbine airfoils, and the crystallographic orientations of both the primary (axial) and secondary (normal to blade axis) airfoil axes should be carefully controlled to best accommodate strains along the airfoil and in the root section. Although the toughness of NiAl is higher at the airfoil-operating temperature, the fracture behavior under impact-loading conditions may still be a concern.

Of more general concern, a low defect tolerance is likely to exist in NiAl; and the size, type, and location of defects become important in components made from NiAl. Internal defects, such as inclusions and porosity, may originate from processing, while machining may introduce surface defects such as scratches, grinding marks, and cracks. Although postprocessing treatments such as hot isostatic pressing (HIP) and electropolishing have been employed to reduce the number and size of defects in NiAl, the limited data available preclude unambiguous conclusions regarding whether these procedures are beneficial. In addition to quantifying and reducing the defect population in NiAl components, design methodologies which can account for the size, type, and location of defects likely to be encountered in the part must be established. The design database must include not only properties determined on laboratory specimens and subcomponents, but also properties from component testing in a variety of simulated conditions on parts with actual configurations. These parts must be made utilizing the same processes which will be used in production in order to reproduce reliably the defect distributions of manufactured hardware. For example, dovetail testing on NiAl blades with actual dovetail geometries has been successfully carried out to alleviate the concerns of low ductility in the attachment area (Darolia *et al.*, 1992c).

The design of the blade should utilize the minimum among the fluctuations in properties, and not the average properties. Design safety margins will depend on the criticality of the part in the total system, and allowed safety factors will be greater than for ductile metals until an experience base for alloys such as NiAl with limited ductility and damage tolerance is established.

3.2 Impact Resistance and Strain-Rate Sensitivity

The DBTT, strain-to-failure, and yield stress of NiAl are relatively constant over the strain rates typically encountered in a turbine engine during normal operation (Lahrman *et al.*, 1991), as presented in Section 2. However, much higher strain rates can be encountered in an impact situation, or when the rotating turbine blades rub against the stationary turbine seals. Although very little information is available concerning the impact resistance of NiAl (Russell *et al.*, 1991; Nardone *et al.*, 1990), many intermetallic compounds fail in a brittle manner even at temperatures above the DBTT. A critical need exists to quantify the impact properties of NiAl over a wide range of temperatures, strain rates, impact angles, and microstructural conditions. Since alloying is unlikely to improve significantly the impact resistance of NiAl, design methodologies which can accommodate the low impact resistance of NiAl need to be established.

3.3 Anisotropic Behavior

The modulus of NiAl is the only relevant basic physical property which shows significant anisotropy; the coefficients of expansion and thermal conductivity are not anisotropic, as expected from the cubic symmetry of NiAl. The modulus has a strong effect on the low- and high-cycle fatigue response of the airfoil, although the magnitude of this effect diminishes slightly near 1000 °C. As described in Section 2, the mechanical properties of NiAl single crystals, specifically the strength and ductility, are much more anisotropic than those of typical Ni-based superalloys. This is true since a single-crystal orientation exists for which the preferred slip systems have zero resolved shear stress, a situation that cannot be produced in typical practical materials such as Ni-based superalloys. However, the magnitude of the anisotropy in ductility becomes small above about 600 °C, and the strength anisotropy diminishes above about 800 °C. While orientations (both primary and secondary) can be specified for independently improving the creep and stress-rupture response, fatigue behavior, strength, and ductility of NiAl single-crystal airfoils,

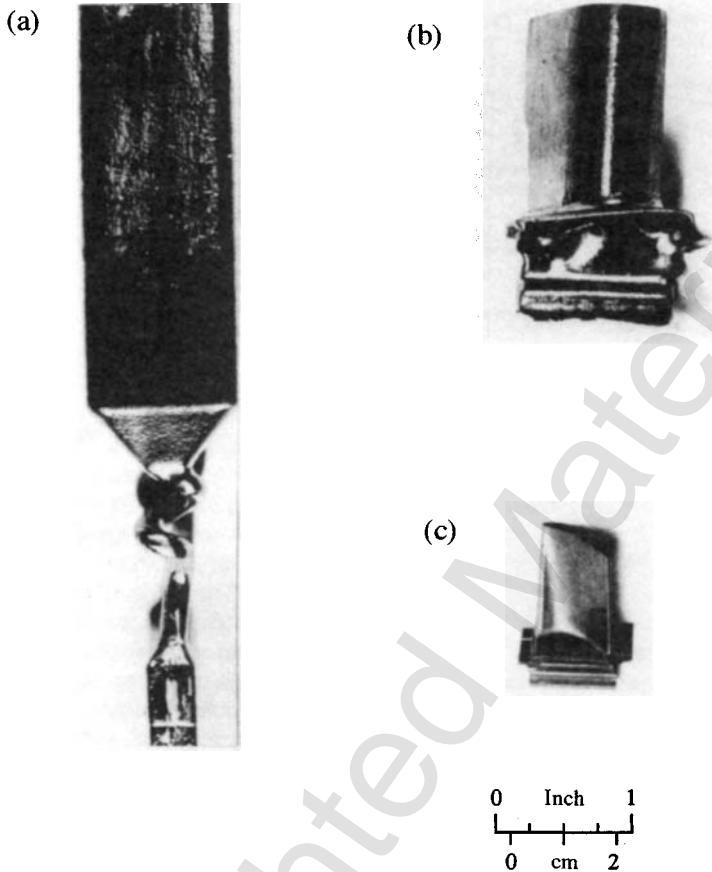


Figure 12. (a) A typical $2.5 \text{ cm} \times 4 \text{ cm} \times 12 \text{ cm}$ NiAl single crystal. (b) A solid, near-net-shape NiAl single-crystal airfoil produced by a modified Bridgman process. (c) A small, single-crystal, high-pressure turbine blade machined from a single-crystal bar (Darolia *et al.*, 1992a)

compromises will have to be made to provide an optimum balance of these competing requirements.

4. Processing, Fabrication, and Machining

Due to the high ductility and low flow stress of binary NiAl above 600°C , conventional thermomechanical processes, such as hot isostatic pressing (HIP) and hot pressing of powder compacts, extrusion, hot rolling, forging, and swaging have been successfully applied to NiAl. However, directional solidification and single-crystal growth are currently the preferred processing routes for turbine blades and vanes, since the elimination of grain boundaries is necessary to obtain adequate high-temperature creep strength. Single-crystal bars of NiAl alloys up to $4 \text{ cm} \times 4 \text{ cm}$ in cross-section have been produced by a modified Bridgman technique

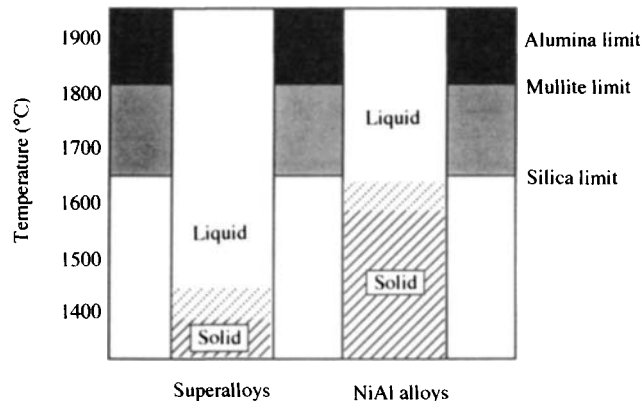


Figure 13. Temperature limits for investment casting mold and core materials with respect to the melting ranges for Ni-based superalloys and NiAl alloys (Darolia *et al.*, 1992a)

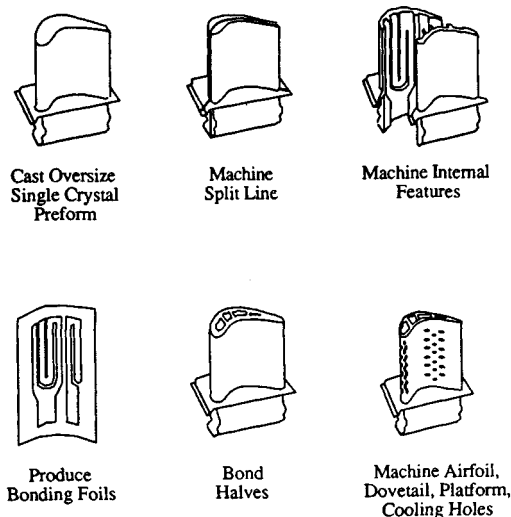


Figure 14. Fabricated blade processing sequence (Darolia *et al.*, 1992a)

(Darolia, 1991; Darolia *et al.*, 1992a). A typical 2.5 cm × 4 cm × 12 cm single crystal is shown in Figure 12(a), and a near-net-shape solid NiAl single-crystal blade is shown in Figure 12(b). A small, single-crystal, high-pressure turbine blade machined from a single-crystal bar is shown in Figure 12(c). Float-zone processes, Czochralski crystal growth, and modified, edge-defined, film-fed growth (where a shaped crystal is grown by drawing liquid metal through a shaped die) have also successfully produced NiAl single crystals, although size limitations with these three processes have not yet been overcome.

The major challenge in producing single crystals of NiAl alloys is the high melting temperature, which is roughly 300 °C higher than the most advanced Ni-based superalloys. In addition to making furnace-related issues more complex (temperature capability, furnace durability, and temperature measurement and control), the higher processing temperatures approach the limits of existing ceramic mold and core materials in terms of structural capability and reactivity with molten NiAl (Figure 13). While large NiAl single-crystal bars and airfoil shapes can be made using the modified Bridgman process, casting of hollow, thin-walled structures has not been demonstrated. The limited low-temperature plasticity of most NiAl alloys, combined with the strains generated when the metal shrinks around the ceramic core during cooling from the casting temperature, results in severe cracking of the metal. Also, core-related problems such as shift, sag, breakage and reactivity are

a major source of low yields in casting superalloy turbine blades in advanced designs, and are anticipated to be a major technical challenge for advanced single-crystal NiAl airfoils.

As an alternative to cast and cored single-crystal blades, a fabricated airfoil approach (Figure 14) is being evaluated to produce complex, thin-walled NiAl alloy turbine airfoils (Darolia *et al.*, 1992a; Goldman, 1992). In this process, a single-crystal preform is split by wire EDM to produce two single-crystal 'matching halves'. Internal cooling passages are machined into each half by electrode EDM or other methods, and the two halves are bonded back together by a process which produces a single crystal across the joint. Single-crystal bond joints, with properties equivalent to the base metal, have been produced in NiAl single crystals using an activated diffusion-bonding process similar to those used for Ni-based superalloys (Goldman, 1992). Finish machining of the airfoil contours and other external blade features is performed, and film-cooling holes are drilled by a combination of mechanical and electrochemical processes. This fabricated blade approach can result in improved dimensional tolerances and improved inspectability, while allowing the freedom to incorporate advanced cooling designs.

Many conventional and nonconventional material removal techniques (grinding, EDM, electrochemical machining, chemical milling, electrostream drilling, ultrasonic machining, abrasive waterjet) have been used on NiAl alloys (Goldman, 1992). Low-stress processes such as EDM, electrochemical milling, chemical milling, and ultrasonic machining are preferred to accommodate the low RT plasticity of NiAl. The recrystallized layer generated by the EDM process has been removed by subsequent chemical milling. Processes such as laser drilling which generate high thermal gradients should be avoided (Goldman, 1992).

A number of manufacturing-related challenges must be addressed to enable the successful application of the fabricated airfoil approach. Methods to control the propagation of positioning errors must be established, including tight control of machining tolerances between the two matching halves of the blades, control of the alignment between the two halves during the bonding cycle (up to 1400 °C), and careful design of a reference datum to allow for precise positioning of the single-crystal halves between the fabrication steps. In-process control and inspection of the crystallographic orientation between the two halves need to be established within a few degrees to obtain parent-metal properties in a bonded blade (Jang *et al.*, 1986). In-process controls and detection methods for both internal and surface

defects need to be established. Computerized tomography, termed XIM (X-ray inspection module), has been used successfully to detect bond-line defects in NiAl (Goldman, 1992).

5. Concluding Remarks

Alloys based on NiAl offer significant potential payoffs as structural materials in gas-turbine applications due to a unique range of physical and mechanical properties. These properties include high melting temperature, low density, high thermal conductivity, excellent environmental resistance, and anisotropic elastic and plastic properties. Excellent progress has been made in understanding these properties in binary NiAl, and significant improvements in the strength and ductility of NiAl single crystals have been achieved through alloying. Tensile strength and stress-rupture properties which compete with current Ni-based superalloys have been achieved through precipitation of an ordered L₂ Heusler phase in NiAl single crystals. An RT tensile ductility as high as 6% has been produced in NiAl single crystals containing less than 0.5% (atomic) of Fe, Ga, or Mo. However, a single alloy with both RT ductility and sufficient high-temperature strength has not yet been developed, and may prove to be an elusive goal. While activity to develop an alloy with both high-temperature strength and RT ductility continues, the current approach also emphasizes design and test methodologies which can accept a material with limited ductility and damage tolerance. More work is required on measuring and understanding strain-rate sensitivity and impact behavior. While several significant challenges still remain, excellent progress has been made in many areas, and the prognosis for using NiAl alloys as high-temperature structural materials is promising.

6. Acknowledgements

We would like to acknowledge several of our colleagues who have contributed to the progress made on NiAl. They are R. D. Field, D. F. Lahrman, J. R. Dobbs, E. H. Goldman, W. S. Walston, K. Bain, P. K. Wright, J. C. Nickley, and D. G. Konitzer of General Electric Aircraft Engines; K.-M Chang of General Electric Corporate Research and Development Center; M. V. Nathal of NASA Lewis Research Center; K. Vedula of the Iowa State University; and R. Gibala of the University of Michigan. Portions of the work reported in this chapter were supported under the Independent

Research and Development projects at GE Aircraft Engines, and by the Air Force Office of Scientific Research (A. H. Rosenstein, Air Force Wright Laboratory (W. A. Troha, M. J. Kinsella, and R. H. Lilley), and the Naval Air Propulsion Center (A. S. Culbertson).

7. References

- Au, Y. K., and Wayman, C. M. (1972). *Scripta Metall.*, **6**, 1209.
- Ayushina, G. D., Levin, E. S., and Gel'd, P. V. (1969). *Russ. J. Phys. Chem.*, **43**, 1548.
- Bain, K. (1992a). Unpublished research under Air Force Contract F33615-90-C-9008, General Electric Aircraft Engines, Cincinnati, OH.
- Bain, K. (1992b). In *Intermetallic HP Turbine Technology Development*, Phase I Interim Report. Air Force Contract F33615-90-C-2006, WL-TR-92-2016, AF Wright Laboratory.
- Baker, I., Nagpal, P., Liu, F., and Munroe, P. R. (1991). *Acta Metall. Mater.*, **39**, 1637.
- Ball, A., and Smallman, R. E. (1966a). *Acta Metall.*, **14**, 1517.
- Ball, A., and Smallman, R. E. (1966b). *Acta Metall.*, **14**, 1349.
- Barrett, C. L. (1988). *Oxid. Met.*, **30**(5/6), 361–390.
- Bevk, J., Dodd, R. A., and Strutt, P. R. (1973). *Metall. Trans.*, **4**, 159.
- Boone, D. H., and Goward, G. W. (1970). In *Ordered Alloys—Structural Applications and Physical Metallurgy*, Proceedings 3rd Bolton Landing Conference (eds B. Kear, C. T. Sims, N. S. Stoloff, and J. H. Westbrook). Claitor's Pub. Div., Baton Rouge, p. 545.
- Bowman, R., Noebe, R., and Darolia, R. (1989). In *HITEMP Review*, NASA Conference Publication 10039, 47-1.
- Bradley, A. J., and Taylor, A. (1937). *Proc. R. Soc. London, Ser. A*, **159**, 56.
- Campany, R. G., Loretto, M. H., and Smallman, R. E. (1973). *J. Microsc.*, **98**, 174.
- Chakravorty, S., and Wayman, C. M. (1976a). *Metall. Trans.*, **7A**, 555.
- Chakravorty, S., and Wayman, C. M. (1976b). *Metall. Trans.*, **7A**, 569.
- Chandrasekaran, M., and Mukherjee, K. (1974). *Mater. Sci. Eng.*, **14**, 97.
- Chang, K.-M., Darolia, R., and Lipsitt, H. A. (1991). In *High Temperature Ordered Intermetallic Alloys IV* (eds L. A. Johnson, J. O. Stiegler, and D. P. Pope). *MRS Proc.*, **213**, 597.
- Clapp, P. C., Rubins, M. J., Charpenay, S., Rifkin, J. A., and Yu, Z. Z. (1989). In *High Temperature Ordered Intermetallic Alloys III* (eds C. T. Liu, A. I. Taub, N. S. Stoloff, and C. C. Koch). *MRS Proc.*, **133**, 29.
- Clark, R. W., and Whittenberger, J. D. (1984). In *Proceedings of the 8th International Thermal Expansion Symposium* (ed. T. A. Hahan). Plenum Press, New York, p. 189.
- Dannohl, H.-D., and Lukas, H. L. (1974). *Z. Metallk.*, **65**, 642.
- Darolia, R. (1991). *J. Met.*, **43**(3), 44.

- Darolia, R., and Chang, K.-M. (1991). Independent research and development program, General Electric Aircraft Engines.
- Darolia, R., Lahrman, D. F., Field, R. D., Dobbs, J. R., Chang, K.-M., Goldman, E. H., and Konitzer, D. G. (1992a). In *Ordered Intermetallics—Physical Metallurgy and Mechanical Behavior*, Vol. 213 (eds C. T. Liu, R. W. Cahn, and G. Sauthoff). NATO ASI Series E: Applied Sciences. Kluwer Academic, Dordrecht, p. 679.
- Darolia, R., Lahrman, D. F., and Field, R. (1992b). *Scripta Metall. Mater.*, **26**, 1007.
- Darolia, R., Walston, W. S., and Lahrman, D. (1992c). Unpublished research, General Electric Aircraft Engines, Cincinnati, OH.
- Doychak, J., Smialek, J. L., and Barrett, C. A. (1989). In *Oxidation of High Temperature Intermetallics* (eds T. Grobstein and J. Doychak). TMS, Warrendale, PA, pp. 41–55.
- Enami, K., and Nenno, S. (1971). *Metall. Trans.*, **2**, 1487.
- Enami, K., Nenno, S., and Shimizu, K. (1973). *Trans. Jpn Inst. Met.*, **14**(2), 161.
- Epperson, J. E., Gerstenberg, K. W., and Berner, D. (1978). *Philos. Mag. A*, **38**, 529.
- Ettenberg, M., Komarek, K. L., and Miller, E. (1970). In *Ordered Alloys—Structural Applications and Physical Metallurgy*, Proceedings 3rd Bolton Landing Conference (eds B. Kear, C. T. Sims, N. S. Stoloff, and J. H. Westbrook). Claitor's Pub. Div., Baton Rouge, p. 49.
- Field, R. D. (1991). Unpublished research, General Electric Aircraft Engines, Cincinnati, OH.
- Field, R. D. (1992a). In *Intermetallic HP Turbine Technology Development*, R&D Status Report 8. Air Force Contract F33615-90-C-2006, AF Wright Laboratory.
- Field, R. D. (1992b). In *Intermetallic HP Turbine Technology Development*, Phase I Interim Report. Air Force Contract F33615-90-C-2006, WL-TR-92-2016, AF Wright Laboratory.
- Field, R. D., Darolia, R., Lahrman, D. F., and Freeman, A. J. (1991). In *Alloy Modeling and Experimental Correlation for Ductility Enhancement in Near Stoichiometric Single Crystal Nickel Aluminide*, Final Report. AFOSR Contract F49620-88-C-0052, Bolling AFB, Washington, DC.
- Field, R. D., Lahrman, D. F., and Darolia, R. (1991a). In *High Temperature Ordered Intermetallic Alloys IV* (eds L. A. Johnson, J. O. Stiegler, and D. P. Pope). *MRS Proc.*, **213**, 255.
- Field, R. D., Lahrman, D. F., and Darolia, R. (1991b). *Acta Metall. Mater.*, **39**, 2951.
- Field, R. D., Lahrman, D. F., and Darolia, R. (1991c). *Acta Metall. Mater.*, **39**, 2961.
- Forbes, K. R., Glatzel, U., Darolia, R., and Nix, W. D. (1993). Presented at the MRS Symposium on Ordered Intermetallic Alloys V, Boston, p. 45.
- Fox, A. G., and Tabernor, M. A. (1991). *Acta Metall. Mater.*, **39**, 669.
- Fraser, H. L., Loretto, M. H., and Smallman, R. E. (1973a). *Philos. Mag.*, **28**, 667.
- Fraser, H. L., Smallman, R. E., and Loretto, M. H. (1973b). *Philos. Mag.*, **28**, 651.
- Fu, C. L., and Yoo, M. H. (1991). In *High Temperature Ordered Intermetallic Alloys IV* (eds L. A. Johnson, J. O. Stiegler, and D. P. Pope). *MRS Proc.*, **213**, 667.
- George, E. P., and Liu, C. T. (1990). *J. Mater. Res.*, **5**, 754.
- George, E. P., Liu, C. T., and Liao, J. J. (1990). In *Alloy Phase Stability and Design* (eds G. M. Stocks, A. F. Giamei, and D. P. Pope). *MRS Proc.*, **186**, 375.
- Goldman, E. H. (1992). In *Advanced NiAl Turbine Blade*, Phase I Interim Report. Air Force Contract F33615-90-C-5938, AF Wright Laboratory.
- Goward, G. W. (1970). *J. Metal.*, **22**(10), 31.
- Grala, E. M. (1960). In *Mechanical Properties of Intermetallic Compounds* (ed. J. H. Westbrook). John Wiley & Sons Ltd, New York, p. 358.
- Guard, R. W., and Turkalo, A. M. (1960). In *Mechanical Properties of Intermetallic Compounds* (ed. J. H. Westbrook). John Wiley & Sons Ltd, New York, p. 141.
- Hahn, K. H., and Vedula, K. (1989). *Scripta Metall.*, **23**, 7.
- Hancock, G. F., and McDonnell, B. R. (1971). *Phys. Stat. Sol. (A)*, **4**, 143.
- Harmouche, M. R., and Wolfenden, A. (1987). *J. Test. Eval.*, **15**(2), 101.
- Henig, E.-T., and Lukas, H. L. (1975). *Z. Metallk.*, **66**, 98.
- Hocking, L. A., Strutt, P. R., and Dodd, R. A. (1971). *J. Inst. Met.*, **99**, 98.
- Hong, T., and Freeman, A. J. (1991a). *Phys. Rev. B*, **43**, 6446.
- Hong, T., and Freeman, A. J. (1991b). Unpublished research, Northwestern University, Chicago, IL.
- Hughes, T., Lautenschlager, E. P., Cohen, J. B., and Brittain, J. O. (1971). *J. Appl. Phys.*, **42**, 3705.
- Hutchings, R., and Loretto, M. H. (1978). *Met. Sci.*, **12**, 503.
- Jang, H., Eichelberger, P. M., and Wright, P. K. (1986). In *Fatigue and Fracture of Fabricated Turbine Blades*, Final Report. Air Force Contract F33615-83-5041, AFWAL-TR-86-4073, AF Wright Laboratory.
- Jedlinski, J., and Mrowec, S. (1987). *Mater. Sci. Eng.*, **87**, 281.
- Jha, S. C., Ray, R., and Gaydos, D. J. (1989). *Scripta Metall.*, **23**, 805.
- Kim, J. T. (1991). PhD dissertation, University of Michigan.
- Kumar, K. S. (1991). *ISIJ Int.*, **31**, 1249.
- Kumar, K. S., Darolia, R., Lahrman, D., and Mannan, S. K. (1992b). *Scripta Metall. Mater.*, **26**, 1001.
- Kumar, K. S., Mannan, S. K., and Viswanadham, R. K. (1992a). *Acta Metall. Mater.*, **40**, 1201.
- Lahrman, D. F. and Darolia, R. (1992). In *Intermetallic HP Turbine Technology Development*, Phase I Interim Report. Air Force Contract F33615-90-C-2006, WL-TR-92-2016, AF Wright Laboratory.
- Lahrman, D. F., Field, R. D., and Darolia, R. (1991). In *High Temperature Ordered Intermetallic Alloys IV* (eds L. A. Johnson, J. O. Stiegler, and D. P. Pope). *MRS Proc.*, **213**, 603.
- Lasalmonie, A., Lequeux, M. J., and Costa, P. (1979). In *Strength of Metals and Alloys: Proceedings of the 5th International Conference*, Vol. 2 (eds P. Haasen, V. Gerold, and G. Kostorz). Pergamon Press, New York, p. 1317.

- Lautenschlager, E. P., Kiewit, D. A., and Brittain, J. O. (1965). *Trans. Metall. Soc. AIME*, **233**, 1297.
- Law, C. C. and Blackburn, M. J. (1987). In *Rapidly Solidified Lightweight Durable Disk Materials*. AFWAL TR-87-4102, AF Wright Laboratory.
- Lewandowski, J. J., Michal, G. M., Locci, I., and Rigney, J. D. (1990). In *Alloy Phase Stability and Design* (eds G. M. Stocks, A. F. Giamei, and D. P. Pope). *MRS Proc.*, **186**, 341.
- Locci, I. E., Dickerson, R., Bowman, R. R., Whittenberger, J. D., Nathal, M. V., and Darolia, R. (1992). Presented at the MRS Symposium on Ordered Intermetallic Alloys V, Boston, p. 635.
- Locci, I. E., Noebe, R. D., Bowman, R. R., Minor, R. V., Nathal, M. V., and Darolia, R. (1991). In *High Temperature Ordered Intermetallic Alloys IV* (eds L. A. Johnson, J. O. Stiegler, and D. P. Pope). *MRS Proc.*, **213**, 1013.
- Loretto, M. H. and Wasilewski, R. J. (1971). *Philos. Mag.*, **23**, 1311.
- Lui, S.-C., Davenport, J. W., Plummer, E. W., Zehner, D. M., and Fernando, B. W. (1990). *Phys. Rev. B*, **42**, 1582.
- McCarron, R. L., Lindblad, N. R., and Chatterji, K. (1976). *Corrosion*, **32**, 476.
- Miracle, D. B. (1991). *Acta Metall. Mater.*, **39**, 1457.
- Miracle, D. B. (1993). *Acta Metall. Mater.*, **41**, 649.
- Miracle, D. B., Russell, S., and Law, C. C. (1989). In *High Temperature Ordered Intermetallic Alloys III* (eds C. T. Liu, A. I. Taub, N. S. Stoloff, and C. C. Koch). *MRS Proc.*, **133**, 225.
- Moose, C. A. (1991). MS thesis, Pennsylvania State University.
- Mrowec, S., Danielewski, M., Godlewska, E., and Godlewski, K. (1989). In *Oxidation of High Temperature Intermetallics* (eds T. Grobstein and J. Doychak). TMS, Warrendale, PA p. 147.
- Nagasawa, A., Enami, K., Ishino, Y., Abe, Y., and Nenno, S. (1974). *Scripta Metall.*, **8**, 1055.
- Nagpal, P., Baker, I., Liu, F., and Munroe, P. R. (1991). In *High Temperature Ordered Intermetallic Alloys IV* (eds L. A. Johnson, J. O. Stiegler, and D. P. Pope). *MRS Proc.*, **213**, 533.
- Nardone, V. C., Strife, J. R., and Prewo, K. M. (1990). In *Intermetallic Matrix Composites* (eds D. L. Anton, P. L. Martin, D. B. Miracle, and R. McMeeking). *MRS Proc.*, **194**, 205.
- Nash, P., Singleton, M. F., and Murray, J. L. (1991). In *Phase Diagrams of Binary Nickel Alloys*, Vol. 1 (ed. P. Nash). ASM International, Metals Park, OH, p. 3.
- Nathal, M. V. (1992). In *Ordered Intermetallics—Physical Metallurgy and Mechanical Behavior*, Vol. 213 (eds C. T. Liu, R. W. Cahn, and G. Sauthoff). NATO ASI Series E: Applied Sciences. Kluwer Academic, Dordrecht, p. 541.
- Nathal, M. V. and Ebert, L. J. (1985). *Metall. Trans.*, **16A**, 427.
- Neumann, J. P., Chang, Y. A., and Lee, C. M. (1976). *Acta Metall.*, **24**, 593.
- Noebe R. and Whittenberger, J. D. (1991). Unpublished research, NASA–Lewis Research Center, Cleveland, OH.
- Parthasarathi, A. and Fraser, H. L. (1984). *Philos. Mag. A*, **50**, 89.
- Pascoe, R. T. and Newey, C. W. A. (1968). *Met. Sci. J.*, **2**, 138.
- Petrushevskii, M. S., Levin, E. S., and Gel'd, P. V. (1971). *Russ. J. Phys. Chem.*, **45**, 1719.
- Polvani, R. S., Tzeng, W. S., and Strutt, P. R. (1976). *Metall. Trans.*, **7A**, 33.
- Rachinger, W. A. and Cottrell, A. H. (1956). *Acta Metall.*, **4**, 109.
- Raj, S. V., Noebe, R. D., and Bowman, R. R. (1989). *Scripta Metall.*, **23**, 2049.
- Rao, S. I., Woodward, C., and Parthasarathy, T. A. (1991). In *High Temperature Ordered Intermetallic Alloys IV* (eds L. A. Johnson, J. O. Stiegler, and D. P. Pope). *MRS Proc.*, **213**, 125.
- Reuss, S. and Vehoff, H. (1990). *Scripta Metall. Mater.*, **24**, 1021.
- Rigney, J. D., Khadkikar, P. S., Lewandowski, J. J., and Vedula, K. (1989). In *High Temperature Ordered Intermetallic Alloys III* (eds C. T. Liu, A. I. Taub, N. S. Stoloff, and C. C. Koch). *MRS Proc.*, **133**, 603.
- Rosen, S. and Goebel, J. A. (1968). *Trans. Metall. Soc. AIME* **242**, 722.
- Rozner, A. G. and Wasilewski, R. J. (1966). *J. Inst. Metl.*, **94**, 169.
- Rudy, M. and Sauthoff, G. (1985). In *High Temperature Ordered Intermetallic Alloys* (eds C. C. Koch, C. T. Liu, and N. S. Stoloff). *MRS Proc.*, **39**, 327.
- Rudy, M. and Sauthoff, G. (1986). *Mater. Sci. Eng.*, **81**, 525.
- Rusovic, N. and Warlimont, H. (1977). *Phys. Stat. Sol. (A)*, **44**, 609.
- Rusovic, N. and Warlimont, H. (1979). *Phys. Stat. Sol. (A)*, **53**, 283.
- Russell, S. M., Law, C. C., Blackburn, M. J., Clapp, P. C., and Pease, D. M. (1991). In *Lightweight Disk Alloy Development*. WRDC TR-90-4125, AF Wright Research and Development Center.
- Sauthoff, G. (1989). *Z. Metallk.*, **80**, 337.
- Schneibel, J. H., Darolia, R., Lahrman, D. F., and Schmauder, S. (1992). *Metall. Trans.*, submitted.
- Schulson, E. M. (1985). In *High Temperature Ordered Intermetallic Alloys* (eds C. C. Koch, C. T. Liu, and N. S. Stoloff). *MRS Proc.*, **39**, 193.
- Schulson, E. M. and Barker, D. R. (1983). *Scripta Metall.*, **17**, 519.
- Seybolt, A. U. (1966). *Trans. ASM*, **59**, 860.
- Smialek, J. L. and Hehemann, R. F. (1973). *Metall. Trans.*, **4**, 1571.
- Smialek, J. L. and Meier, G. H. (1987). In *Superalloys II* (eds C. T. Sims, N. S. Stoloff, and W. C. Hagel). John Wiley & Sons Ltd, Chichester, pp. 293–326.
- Stover, E. T. (1966). In *Effects of Alloying and Deformation Processing on Mechanical Behavior of NiAl*, WADC-TDR-60-184, Part VII, Vol. II. USAF Contract AF-33(615)-1497, Wright Air Development Center.

- Tanner, L. E., Pelton, A. R., VanTendeloo, G., Schryvers, D., and Wall, M. E. (1990). *Scripta Metall. Mater.*, **24**, 1731.
- Taylor, A. and Doyle, N. J. (1972). *J. Appl. Cryst.*, **5**, 201.
- Vandervoort, R. R., Mukherjee, A. K., and Dorn, J. E. (1966). *Trans. ASM*, **59**, 930.
- Vedula, K., Hahn, K. H. and Boulogne, B. (1989). In *High Temperature Ordered Intermetallic Alloys III* (eds C. T. Liu, A. I. Taub, N. S. Stoloff, and C. C. Koch). *MRS Proc.*, **133**, 299.
- Vehoff, H. (1992). In *Ordered Intermetallics—Physical Metallurgy and Mechanical Behavior*, Vol. 213 (eds C. T. Liu, R. W. Cahn, and G. Sauthoff). NATO ASI Series E: Applied Sciences. Kluwer Academic, Dordrecht, p. 299.
- Veyssi re, P. and Noebe, R. (1992). *Philos. Mag. A*, **65**, 1.
- Wachtell, R. L. (1952). In *Investigation of Various Properties of NiAl*, Technical Report 52-291, Wright Air Development Center.
- Walston, W. S. (1992a). In *Intermetallic HP Turbine Technology Development*, Phase I Interim Report. Air Force Contract F33615-90-C-2006, WL-TR-92-2016, AF Wright Laboratory.
- Walston, W. S. (1992b). In *Intermetallic HP Turbine Technology Development*, R&D Status Report 8. Air Force Contract F33615-90-C-2006, AF Wright Laboratory.
- Walston, W. S. and Darolia, R. (1993). In *High Temperature Ordered Intermetallic Alloys V* (eds I. Baker, R. Darolia, J. D. Whittenberger, and M. H. Yoo). *MRS Proc.*, **288**, 237.
- Wasilewski, R. J. (1966). *Trans. Metall. Soc. AIME*, **236**, 455.
- Wasilewski, R. J. (1968). *J. Phys. Chem. Solids*, **29**, 39.
- Wasilewski, R. J., Butler, S. R., and Hanlon, J. E. (1967). *Trans. Metall. Soc. AIME*, **239**, 1357.
- West, G. W. (1964). *Philos. Mag.*, **9**, 979.
- Westbrook, J. H. (1956). Unpublished research, General Electric CR&D Center, Schenectady, N.Y.
- Whittenberger, J. D. (1987). *J. Mater. Sci.*, **22**, 394.
- Whittenberger, J. D. (1988). *J. Mater. Sci.*, **23**, 235.
- Whittenberger, J. D., Arzt, E., and Luton, M. J. (1990). *J. Mater. Res.*, **5**, 271.
- Whittenberger, J. D., Nathal, M. V., Raj, S. V., and Pathare, V. M. (1991). *Mater. Lett.*, **11**, 267.
- Whittenberger, J. D. and Viswanadham, R. K. (1989). In *High Temperature Ordered Intermetallic Alloys III* (eds C. T. Liu, A. I. Taub, N. S. Stoloff, and C. C. Koch). *MRS Proc.*, **133**, 621.
- Wright, P. K., Maurer, N., and Bain, K. (1992). Unpublished research, General Electric Aircraft Engines, Cincinnati, OH.
- Yaney, D. L. and Nix, W. D. (1988). *J. Mater. Sci.*, **23**, 3088.
- Yang, W. J. and Dodd, R. A. (1973). *Met. Sci. J.*, **7**, 41.

This chapter was originally published in 1995 as Chapter 3 in *Intermetallic Compounds*, Vol. 2: *Practice*, edited by J. H. Westbrook and R. L. Fleischer.